Available online at www.sciencedirect.com
SCIENCE DIRECT
Catalysis Today 105 (2005) 560–568
CATALYSIS TODAY
www.elsevier.com/locate/cattod

Imposing dynamic structures on fluidised beds

F. Kleijn van Willigen *, D. Christensen, J.R. van Ommen, M.-O. Coppens

DelftChemTech, Faculty of Applied Sciences, Delft University of Technology, Julianalaan 136, 2628 BL Delft, The Netherlands

Available online 11 July 2005

Abstract

Structuring fluidised beds can increase the conversion and selectivity, and facilitate control and scale-up. Two methods for introducing a dynamic structure into gas–solid fluidised beds are compared based on their overall hydrodynamics: electric field enhanced fluidisation and distributed secondary gas injection by a fractal injector. It is shown that, under various conditions, these systems lead to significant decreases in bubble size and bubble hold-up and to an increase in the number of bubbles. It was found that the electric field enhancement can lead to homogeneous fluidisation at lower flow rates, and the distributed secondary flow leads to smaller bubbles at higher flow rates.

Keywords: Fluidised beds; Bubble size; Bubble hold-up; Electric fields; Fractal gas injection

1. Introduction

Two common reactor types for heterogeneously catalysed gas phase reactions are the packed bed and the fluidised bed. Fluidised beds couple short intraparticle diffusion lengths to good heat transfer, but suffer from chaotic bubble behaviour [1], leading to back-mixing, fluid bypassing, and particle–fluid separation problems [2]. Packed beds show much less back-mixing and have virtually no catalyst attrition and separation problems, but have longer diffusion lengths that can only be overcome by an unacceptably large pressure drop. Moreover, they are sensitive to flow maldistribution that can lead to problems such as poor catalyst contact, hot-spot formation, and runaway behaviour [3]. In the past few years, much effort has been devoted to the development of reactors in which the catalyst material is present in a static, structured way, e.g., monolith and Katapak® reactors [4]. However, for reactions with large heat production and/or fast catalyst deactivation, it is often advantageous to use a mobile catalyst [2]. In these cases, fluidised beds are preferred, despite the disadvantages of chaotic bubble behaviour and the difficulty of scaling fluidised beds from lab-scale to pilot- and industrial-scale. Just as for packed bed reactors, the structuring of fluidised beds is interesting from the point of view of process intensification, to facilitate scale-up and control, and to improve performance.

In this paper, we will show that it is possible to manipulate the hydrodynamic structure of fluidised-bed reactors, thereby increasing the number of degrees of freedom for the designer, and helping to intensify the process. This is achieved by manipulating the interparticle forces and particle–fluid interactions to obtain the desired fluidisation behaviour for a given application. Two methods of structuring gas–solids fluidised beds are presented and compared: imposing an electric field and secondary injection of gas. By using these non-conventional 'active' internals, we introduce a dynamic structure into the fluidised bed, leading to better control over the hydrodynamics of the system (especially the bubbles). The contact of the gas in bubbles with the solid catalyst particles is often poor, and when the catalyst itself is sufficiently active, the mass-transfer from bubble to emulsion is the rate-limiting step. Therefore, our goal is to *control* the bubble behaviour and *decrease* the average bubble size in a structured manner. A decrease of the bubble diameter by a factor four can increase the conversion in a fluidized bed as much as 2.5 times, and is therefore well worth investigating [5,6].

Three cases are discussed and compared: the base case of a column with no active internals, a column using *electric*

* Corresponding author. Tel.: +31 15 2784753; fax: +31 15 2785006.
E-mail address: F.KleijnvanWilligen@tnw.tudelft.nl
(F. Kleijn van Willigen).

0920-5861/$ – see front matter © 2005 Elsevier B.V. All rights reserved.
doi:10.1016/j.cattod.2005.06.037

field enhanced fluidisation (EF), and a column with secondary gas injection by a *fractal injector* (FI). Using both pressure fluctuation analysis and video analysis of the quasi 2-D column, we attempt to discern the effect of these improvements on the hydrodynamics and bubble behaviour of bubbling fluidised beds.

1.1. Electric field enhanced fluidisation (EF)

One method to reduce bubble size is the application of an AC electric field to a fluidised bed of semi-insulating particles. In the presence of a relatively low intensity electric field, the glass particles in the bed become polarised, leading to attractive or repulsive forces.

The degree of polarisation, P, of particles with a diameter d_p in a fluidised bed dictates the magnitude of the interparticle forces and is a function of the electrical conductivity, σ_e, and the dielectric constants of particle, and continuous phase (ε_p and ε_c), as well as the electric field strength, E_0.

$$P = f(d_p^3, \epsilon_p, \epsilon_c, \sigma_e(\mathrm{RH}), E_0) \quad (1)$$

The conductivity of the system is strongly influenced by the relative humidity, RH, of the fluidising gas.

The influence of small variations in interparticle forces on fluidisation behaviour has been shown both experimentally (e.g., liquid bridges [7], magnetic forces [8], electric polarisation forces, e.g., [9,10]), and in discrete element models (e.g., [11]). The electrical forces thus induced by the electric field should be large enough to decrease the formation and growth of bubbles, but small enough to allow the free movement of particles, i.e., the fluidity of the system must be preserved. The oscillation of the AC fields has the advantage over constant (DC) electric fields that fixation of particles or defluidisation is unlikely.

In practice, the electric fields are introduced in the bed by stringing thin wires through the column (cf. Fig. 1a), and alternately, both horizontally and vertically, driving these with an AC potential or grounding them. This creates a strongly inhomogeneous field in both the horizontal and vertical directions in the column.

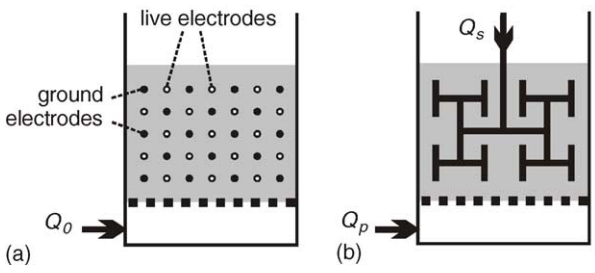

Fig. 1. Two ways of structuring gas–solids fluidised beds with active internals: (a) imposing an AC electric field and (b) secondary (fractal) injection of gas [12].

1.2. Secondary injection of gas using a fractal injector (FI)

The number of degrees of freedom available to optimise the fluidised bed hydrodynamics increases when part of the gas is injected at various other locations inside the bed rather than only feeding the gas via the bottom [12]. This is possible as long as enough "primary" gas (Q_p) is injected from the bottom in order to maintain fluidisation ($Q_p > Q_{mf}$), while an injector distributes the remaining "secondary" gas (Q_s) into the bed. This way, the amounts of gas distributed over the reactor space can be optimally dosed to control both hydrodynamics and reactor performance. Rising gas, depleted of reactants, is continuously replenished with fresh feed. Simultaneously, the bubble size can be controlled, as less primary gas (fraction of primary gas to total gas flow, Q_p/Q_0) leads to smaller bubbles initially, while fresh feed blown into the reactor at various locations (fraction Q_s/Q_0) tends to break up existing bubbles or blow particles apart, leading to an emulsion phase of higher void fraction. Unstable emulsions take time to break up into equilibrated phases, and it is this delay that is exploited. The effects of using secondary gas injection are: increased gas–solid contact due to a higher-than-usual emulsion phase void fraction; smaller, more slowly rising bubbles; and the ability to increase yields and selectivities of chemical processes by a distributed feed. In principle, each injection point could be fed by a separate tube, but it is more useful and practical to connect all injection points by a hierarchical, tree-like fractal structure (cf. Fig. 1b). This gives intrinsic scalability and ensures a uniform access to the smallest branch tips—the outlets. The optimal fractal injector design will depend on the application.

In this paper, we will compare the application of electric fields to the fractal injection of secondary feed, as well as to the baseline cases of a column with inactive internals and a column without internals altogether. The advantages and disadvantages of these two methods of structuring fluidised beds on the hydrodynamics and mass transfer of these systems will be discussed.

2. Experimental

Both columns (EF and FI) were built as similar as possible. By removing the fractal injector from its column, measurements could be conducted in a column without internals. The two quasi-2D Plexiglas columns, 20 cm × 1.5 cm × 80 cm, were fitted with 5 piezo-electric pressure transducers, Kistler type 7261, at 1, 10, 20, and 30 cm above the sintered metal porous distributor, and in the plenum [13]. The pressure drop was measured over the lowest 20 cm of the columns with a Validyne DP15-28. A data acquisition system (LMS-Difa) recorded all measurements at 200 Hz and provided outputs to control the mass flow controllers. The relative humidity (RH) at 1 atm of the

fluidising air was controlled at either 2 or 40% at 30 °C. Baseline measurements were conducted in the column without internals and in the columns with internals but with those internals inactive. The higher RH allowed for enough static charge dissipation that particles did not stick to the walls. The mono-disperse glass beads, $d_p = 550$ μm with a density of 2400 kg/m^3 (Geldart B), were dried in an oven before use, and fluidised at least overnight when the RH was set to 40% before measurements were conducted. The settled bed height was 40 cm. The columns were operated within a cabinet controlled at 30 °C. A digital video camera (25 fps, 576 × 720 pixels) was set up with a viewing window on the column covering an area that spanned from 10 to 40 cm above the distributor. This viewing window was below the bed surface to prevent blinding of the camera by the backlight behind the column.

2.1. Electric field enhanced fluidised bed (EF) set-up

The lower 20 cm of the column were fitted with thin wire electrodes. The wires were threaded through the front and rear of the column at a vertical pitch of 1.25 cm and a horizontal pitch of 2.2 cm. In the horizontal plane, they were threaded diagonally relative to the column walls, so that the nodes of highest field strength are in the centre of the column. The wires were alternately grounded and driven at a potential. The porous metal distributor was also grounded. Frequencies ranging from 1 to 160 Hz (sine wave) and maximum field strengths from 2.4 to 7.2 kV/cm were applied using a Trek 20/20c high voltage amplifier. The LMS-Difa DAQ, besides recording all measurements, served as the signal generator. At least 51200 data points (4.26 min) were measured at every combination of flow rate, field strength, and field frequency. At all the measured field frequencies, a measurement series consisted of a baseline measurement (0 kV applied potential), the range of field strengths, followed by a second baseline measurement. The superficial velocities, as multiples of the minimum fluidization velocity, ranged from 1.5 to 3.5 × u_{mf}, in increments of 0.5 × u_{mf}.

2.2. Fractal injector fluidised bed (FI) set-up

A fractal injector, consisting of 16 uniformly spaced injection points, was constructed from 3 and 6 mm stainless steel tubing and brass connections. Excluding the main feed stem, the fractal injector had the dimensions: 15.6 cm wide by 7.4 cm high, and was centrally positioned in the column at a height of 10 cm above the distributor plate. The highest row of injection points is at approximately 14 cm, and the lowest row at approximately 6 cm. Therefore, the maximum bed height in contact with the fractal injector is somewhat less (∼6 cm) than the EF column. The air fed through the fractal injector is heated but not humidified due to equipment limitations. It is not possible to add enough extra humidity to the primary airflow to make up for this difference and, thus, the humidity of the primary flow was maintained at its normal level (i.e., either the dry plant air or the 40% RH humidified air, depending on the experiment). As a result, the experiments with increasing secondary flow rate unavoidably had decreasing levels of humidity, but never to a level that particle adhesion to the walls or the injector was visible. Experiments were conducted with varying Q_s/Q_p ratios. The total superficial velocities (and therefore flow rates) ranged from 1.5 to 3.5 × u_{mf}, in increments of 0.5 × u_{mf}. At every total flow rate ($Q_s + Q_p$) corresponding to a superficial velocity higher than 1.5 × u_{mf}, Q_s was increased in steps corresponding to 0.5 × u_{mf}, but always with a minimum Q_p corresponding to 1.5 × u_{mf}. At least 204,000 data points (17 min) were measured at every combination of flow rates. Each set of flow conditions always contained a baseline experiment with no secondary flow.

2.3. Data analysis

The analysis of pressure fluctuations is an attractive method to characterize the hydrodynamic behaviour of fluidised beds because the fluctuations are closely associated with properties of the bubbles. Using the pressure probes described earlier, time-series of pressure fluctuations were measured at various heights in the column. A technique proposed by Van der Schaaf et al. [13] was used to decompose the time series into a variance of the pressure time series that is associated with the size of bubbles passing the probe (the incoherent variance, σ^2_{IOP}) and a variance associated with other processes such as the formation, eruption, and coalescence of bubbles (the coherent variance). For more details, the reader is referred to [13]. This method requires measurement of pressure fluctuations in the plenum in addition to the height under consideration. The incoherent variance has been shown to be a good quantitative descriptor of the average bubble size at a certain height in a fluidised bed, although a calibration of this value (for example, using video analysis or optical probes) is required to determine absolute bubble sizes [10]. The measure of bubble size (defined as frontal area of the bubble and, thus, volume for a fixed thickness of the column) derived from pressure fluctuations is theoretically determined by the vertical dimension of the bubble and averaged over long time spans. It does not give information about the total bubble hold-up, or about the number of bubbles. In this study, we are interested in the reduction of average bubble size due to the electric field or fractal injector, and therefore, only consider the ratio of the σ^2_{IOP} in the EF or FI system to the σ^2_{IOP} at normal conditions (baseline with inactive internals).

The second analysis method employed for this comparative study is the use of digital video images. Although not applicable to long experiments (typically only measurements of a few minutes can be properly analysed because of the processing time), video analysis cannot only distinguish the changes in bubble size, like pressure fluctuation analysis, but can also distinguish the changes in the bubble frequency,

which pressure fluctuation analysis cannot. The bubble hold-up can also be determined from video analysis. The video analysis was used as a complementary measurement method only for those settings considered most interesting (i.e., the largest positive influence on the bubble size) based on the pressure fluctuation analysis.

Video analysis over the bed height stretching from 10 to 40 cm was performed for a series of experiments over all flow rates with the most optimal electric field frequency and strength for the EF set-up and the most optimal primary/secondary flow ratio for the FI set-up. For every experiment, 3000 frames (2 min) were recorded. The analysis was carried out in Matlab^{TM}, and consisted of filtering out the background image and the fractal injector stem, then filtering with a median filter and thresholding. The post-processing allows determination of the average bubble size, the bubble frequency and the bubble hold-up as functions of height.

In this study, the bubble size is defined as the area of the face of the bubble in the pseudo-2D column, which implies that bubbles in these columns are essentially voids stretching directly from the front to the back.

3. Results

3.1. Minimum fluidisation

The minimum fluidisation velocity was determined for all set-ups (column without internals, column with wires, column with fractal injector) using pressure drop measurements at both low and elevated RH. The minimum fluidization velocity determined at low RH with the fractal injector present deviated significantly because of adhesion of particles to the walls and the injector due to static charges. For the other cases, the values for u_{mf} were reproducible and found to be $u_{mf} = 21 \pm 1$ cm/s. The column without internals and the column with wires at low RH were less susceptible to particle clinging, perhaps because of small variations in (adsorbed) moisture or age of the particles (attrition), and, therefore, have a more stable minimum fluidization velocity.

3.2. Pressure fluctuation analysis

The pressure fluctuation analysis method was used to find the most optimal strength and frequency of the electric field and the optimal Q_s/Q_p ratio for the fractal injector for the conditions studied. For the EF system, the ratio of the average bubble size under the influence of various strengths to the base case was studied at superficial velocities of 1.5 to $3.5 \times u_{mf}$. The change in bubble size was determined at 20 and 30 cm above the distributor over the whole range of electric field strengths and frequencies, both for the low and elevated relative humidity. Fig. 2 shows the ratio of the bubble size as a function of field strength and frequency to the mean of the base measurements at 20 cm before and after the electric field was switched on. As expected, low field intensities (i.e., less than 4 kV/cm) lead to virtually no change in average bubble size, but at higher field strengths the change in bubble size is very significant.

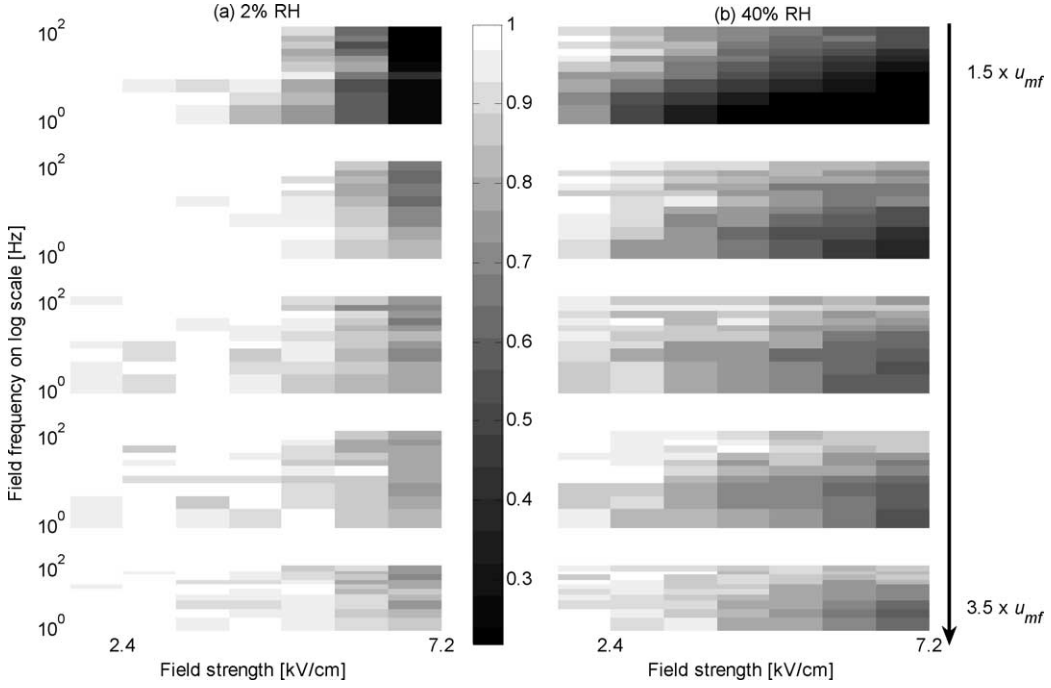

Fig. 2. Ratio of bubble size with applied electric field and without field, as determined by pressure fluctuation analysis at 20 cm above the distributor. (a) 2% RH and (b) 40% RH. The flow rate increases from top ($1.5 \times u_{mf}$) to bottom ($3.5 \times u_{mf}$). Each subplot shows the bubble reduction ratio (cf. the colour scale) as a function of field strength (linear scale) and frequency (logarithmic scale).

Table 1
Ratios of bubble size with most optimal EF and FI to bubble size with passive internals, as determined by pressure fluctuation analysis (σ^2_{IOP})

Superficial velocity ($\times u_{mf}$)	EF optimal frequency (Hz)	σ^2_{IOP} Ratio (30 cm)	σ^2_{IOP} Ratio (20 cm)	FI optimal Q_s/Q_p ratio	σ^2_{IOP} Ratio (30 cm)	σ^2_{IOP} Ratio (20 cm)
1.5	5	0.24	0.08	N/A	N/A	N/A
2.0	5	0.63	0.43	0.5/1.5	0.73	0.49
2.5	10	0.68	0.57	1.0/1.5	0.71	0.42
3.0	5	0.69	0.59	1.5/1.5	0.62	0.36
3.5	5	0.76	0.61	2.0/1.5	0.51	0.30

It has been predicted that the interparticle force increases significantly as the RH increases [14]. As stronger interparticle forces lead to a larger decrease in bubble size, we therefore expect that at a higher RH the bubble size ratio becomes smaller. This is confirmed in the right-hand column of Fig. 2, where the bubble size at, for example, 3.5 × u_{mf}, is decreased by 39% at 20 cm, compared to 28% for the low RH experiment. As the field strength increases, the effect on bubble size also increases, but a dependence on the field frequency is also seen. Especially at the higher RH, lower frequencies lead to larger bubble size decrease, but one must be careful not to defluidise—DC or very low frequency AC fields may gridlock the particles. With increasing flow rate, the net effect of the electric fields becomes smaller and the effect wanes above the electrified region. The optimal electric field frequency was chosen at 10 Hz on the basis of the data presented in Fig. 2, although the results at 5 Hz were slightly better. This was done because low frequencies may lead to particle agglomeration, and the difference in EF efficiency between 5 and 10 Hz was small enough to warrant the choice for higher frequency. The results at optimal frequency and field strength (7.2 kV/cm) are summarized in Table 1.

The pressure fluctuation analysis was also used to estimate the changes in average bubble size in the FI system. This was done at bed heights of 20 and 30 cm over the full range of total flow rates and Q_s/Q_p ratios at both humidity levels. Fig. 3 shows the effect of increasing the Q_s/Q_p ratio at the various total flow rates. It is apparent from the graph that at any total flow rate the bubble size based on incoherent variance decreases with increasing Q_s/Q_p ratio. This trend is consistent at both bed heights, but is slightly less pronounced at the higher height due to bubble coalescence, i.e., the effect of the secondary injection is beginning to wane as the bed tries to return to its equilibrium state. The largest change in bubble size (represented by lower numbers in Table 1 and Fig. 3) always occurs at the highest secondary flow rates and also at the highest total flow rates.

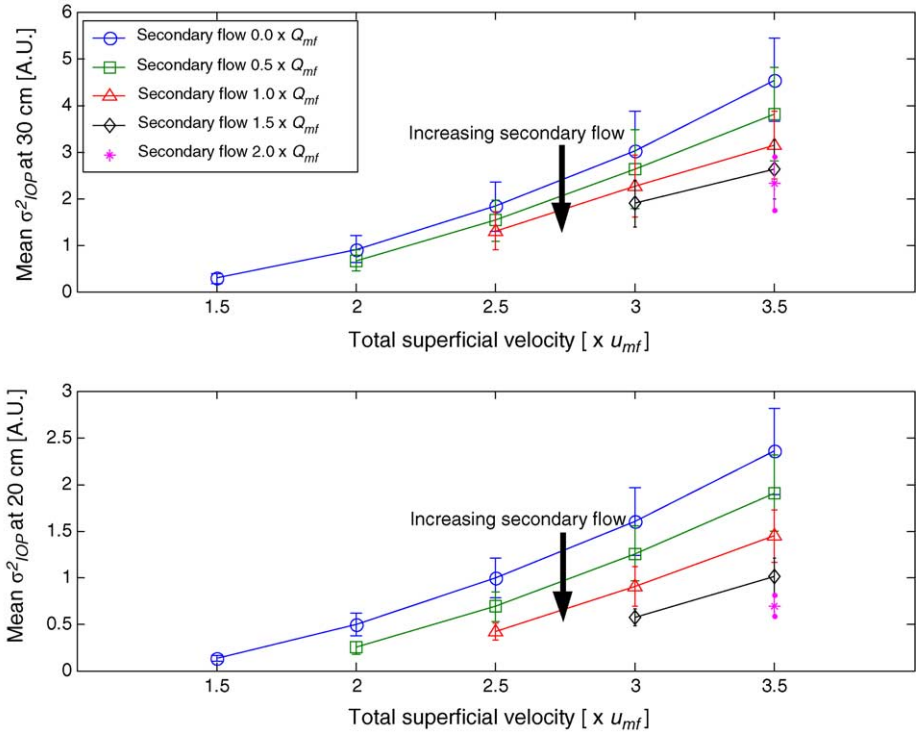

Fig. 3. Effect of increasing the ratio of secondary to primary flow on the incoherent variance, when using the set-up with fractal injector, as a function of total flow rate. The σ^2_{IOP} is a measure for bubble size based on pressure fluctuation analysis. Measurements carried out at 40% RH.

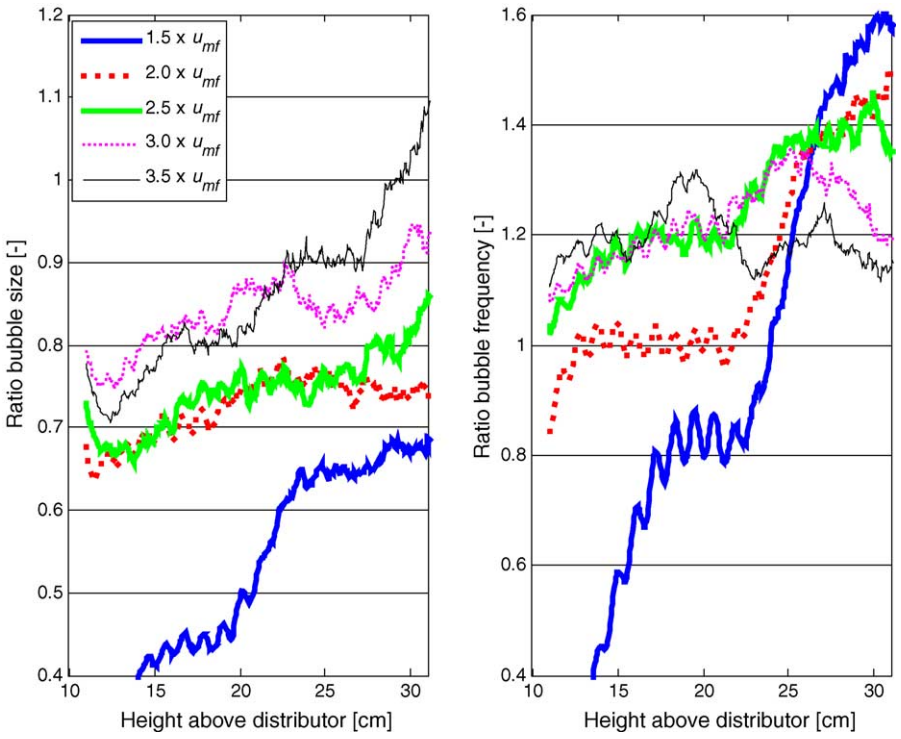

Fig. 4. The relative bubble size (a) and frequency (b) under the effect of the electric fields, determined using video analysis. The electric fields reduce the bubble size and, at higher flow rates, increase the number of bubbles. Measurements carried out at 40% RH. The electrodes end 20 cm above the distributor.

Due to the inconsistent humidity levels, as was mentioned earlier, the effect of moisture could not be determined quantitatively. When the secondary flow stream was at its highest, the lowest RH of the combined stream (when humidified) was 17%, compared to 2% for the dry case. However, it will be shown later on the basis of bubble hold-up that there is some influence on the results that is attributed to the relative humidity and how the RH is controlled.

3.3. Video analysis

Video analysis was used to determine average bubble size, frequency and hold-up in the EF and FI systems at the most optimal settings, over the full range of flow rates. This was done at 40% RH. Fig. 4 shows the ratios of average bubble size and the bubble frequency as a function of height for the EF system. As already shown by the pressure fluctuation analysis, the ratio of bubble size with and without electric field decreases, and this is most prominent in the electrified region. In the region above the electrodes, the bubble size at low flow rates stays low, but at higher flow rates, bubbles grow quickly. Nevertheless, within the electrified region, the bubble size is 10–60% smaller, and up to 35% smaller above the wires.

The effect of the electric field on the bubble frequency is shown in Fig. 4b, again as a ratio of bubble frequency with and without applied field. At low flow rates, the bubble frequency within the electrified region is decreased significantly. This is because bubbles are either non-existent or are too small to be detected by the video camera. There is also an oscillation in the bubble frequency due to the direct effect of the field on the bubbles. The number of bubbles in the region above the electrodes is increased by 10–70%, depending on flow rate. The emulsion phase can no longer contain as much gas as it is forced to in the electrified region, and thus, many small bubbles are formed. As visually observed during experiments and confirmed by the lack of bubbles, at the lower flow rates almost homogeneous fluidisation is achieved in the electrified region.

The video analysis results for each total flow rate using the best Q_s/Q_p ratios in the FI system are shown in Fig. 5. Above the internals, it is apparent that the bubble size is smaller and the bubble frequency higher, when compared to the baselines. Just as for the pressure signal analysis, the bubble size ratio decreases with increasing flow rate, while the number of bubbles increases with increasing flow rate. This means that the FI system is more efficient at higher flow rates. Bubble size reductions are all in the range of 15–55% when measured at the same heights as in the pressure signal analysis. The bubble size ratios increase slightly with increasing height due to bubble coalescence while the system tries to return to its equilibrium state. This is corroborated by the slight decrease in bubble frequency over the same region. The fact that the bubble frequency ratio never returns to unity implies that bubble coalescence is delayed by the use of the fractal injector and that a maximum bubble size is not reached (as is expected with Geldart B particles). Results within the region containing the fractal

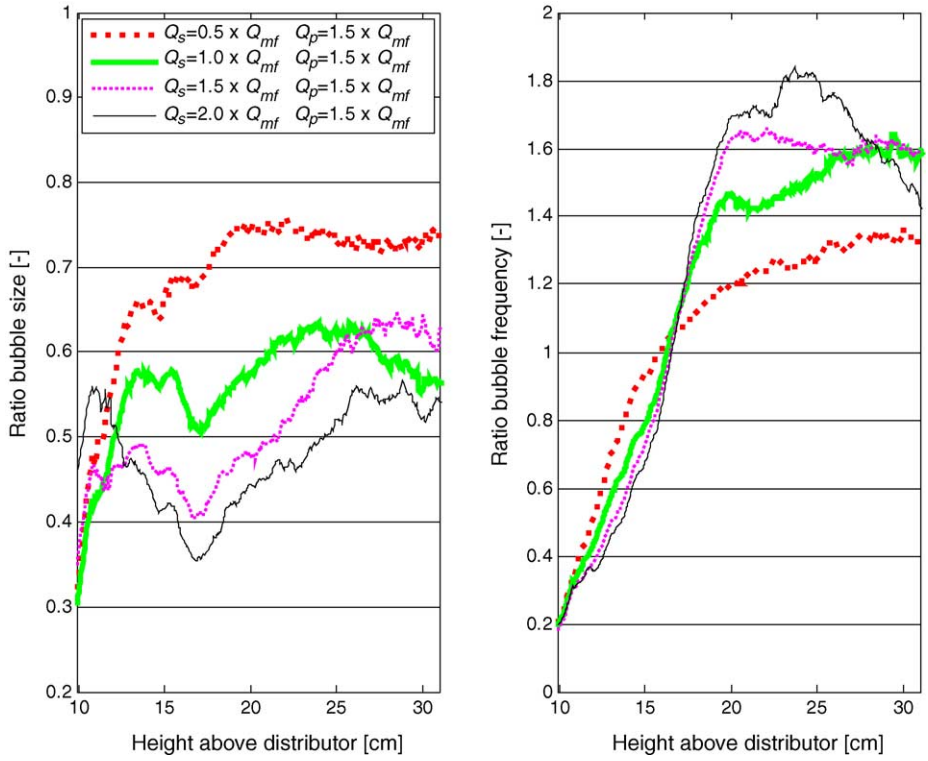

Fig. 5. The effect of the fractal injector on bubble size (left) and bubble frequency (right). The primary flow rate is held constant, the secondary flow increases—this is the most optimal setting. Measurements carried out at 40% RH. The top injection point of the fractal injector is 14 cm above the distributor.

injector are difficult to interpret, as the total gas throughput is changing in this region.

4. Discussion and comparison

Both of the systems presented here were designed to improve bubbling fluidised bed efficiency and both are inherently scalable. In the design of both internals, however, there is much room for optimisation: the spatial distribution of injection points for the fractal injector, and the electrodes in the EF system for highest average field density, as well as an extension of the electrodes to the whole bed height. It should be noted, however, that the introduction of internals into a fluidised bed can be problematic due to attrition. The lifetime of the wires of the EF column is obviously lower than the sturdier fractal injector design, but, on the other hand, the volume density of the wires is much lower than the volume the fractal injector occupies (EF: 0.008%, FI: 1.67%). In addition, the electric field may be introduced using (adaptations of) existing internals or electrodes that are more robust.

Fig. 6 compares the average bubble sizes determined by pressure fluctuation analysis for all different systems: a column without any internals, a column fitted with electrodes, and a column fitted with the fractal injector. Data are compared with both passive and active internals, at elevated RH. The base lines at 30 cm are not significantly different. At 20 cm, the influence of the (passive) fractal injector breaking up bubbles is seen to be significant, causing an estimated 12% bubble size reduction at the highest flow rate. The influence of the wires on bubble behaviour in the EF system is not discernable. When active, both systems are able to reduce bubble size considerably, as already shown in Table 1. The EF system is more effective at the lower flow rates; the FI system gives a larger bubble size reduction at the higher flow rates.

At this point it is most interesting to compare the bubble hold-up of both systems because of the large influence on the effectiveness of the system. A larger amount of gas in the bubble phase means less contact between catalyst particles and gas, usually reducing conversion. Conversely, when the average bubble size decreases and the average number of bubbles in the system increases, an equal or lower bubble hold-up means an increase in the emulsion phase flow (as larger bubbles rise more quickly than small ones, which leads to a lower hold-up). The changes in bubble hold-up of the EF and FI systems are compared in Fig. 7. It is again clear that the EF system is most efficient within the electrified region, leading to a large decrease in bubble hold-up in the lower 20 cm of the column, especially at low flow rates. The bubble hold-up in the same region in the FI column appears to decrease the most at *high* flow rates (large secondary flow), but this is because the total flow at this point is much lower than the reference situation, in which the total flow is all primary flow.

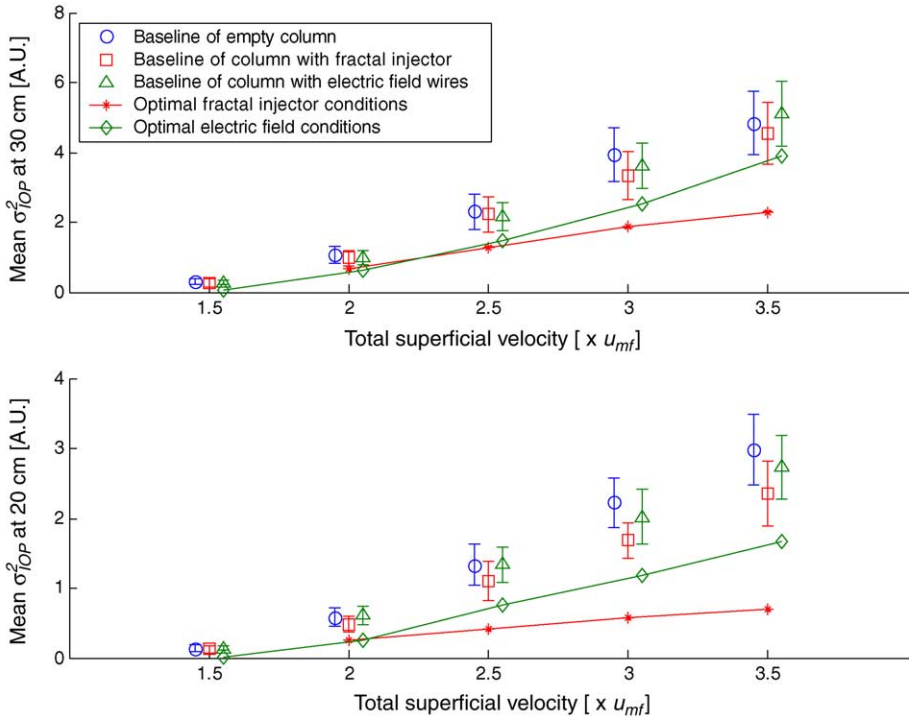

Fig. 6. The pressure fluctuation analysis method applied to the EF and FI measurements at the optimal electric field or secondary flow ratios, as a function of total flow rate. The σ^2_{IOP} is a measure of the mean bubble size. The three baseline measurements show larger bubble sizes than the EF and FI measurements. Data points have been slightly offset along the horizontal axis for clarity and lines were drawn to guide the eye. Error bars denote 95% confidence intervals.

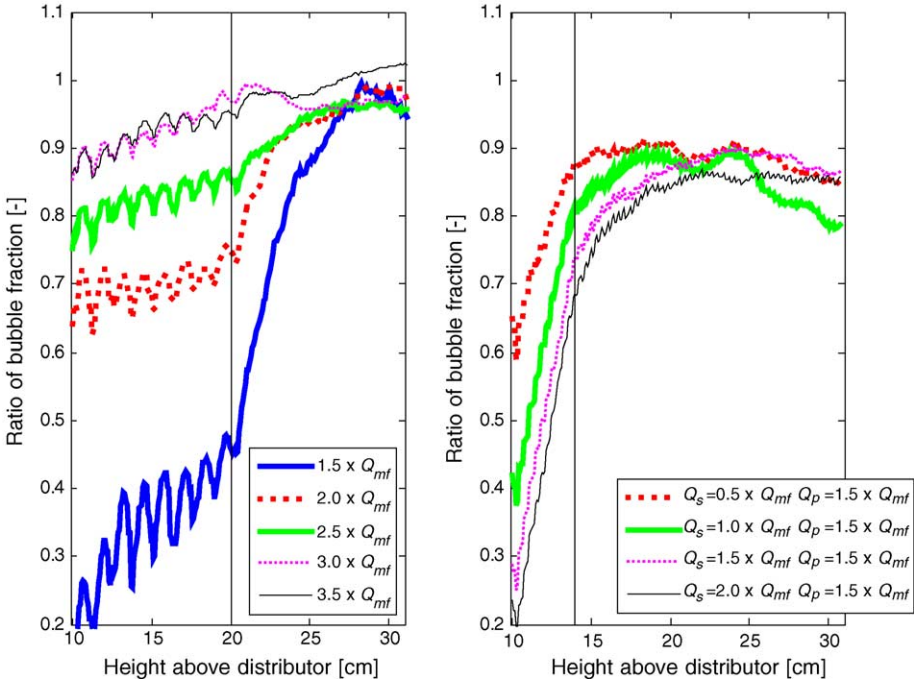

Fig. 7. Comparison of the improvement in bubble hold-up in the EF (left) and FI (right) systems. The vertical lines indicate the top of the internals. The EF and FI internals both decrease bubble hold-up and increase emulsion phase flow. The electric field has only limited influence on the region above the electrodes, while the FI shows a longer lasting effect. A decrease in bubble hold-up, combined with more and smaller (slower travelling) bubbles, implies an increase in emulsion phase flow.

In the region of 20–30 cm above the distributor, the influence of the electric fields quickly decays—the bubble hold-up is 90–100% of the baseline values, with some overshoot at the highest flow rate. However, the FI appears to maintain its effect by keeping the bubble hold-up to 80–90% of the baseline values. This difference in bubble hold-up is high, and the increase in emulsion flow may contribute only to part of the decrease. A more detailed study of the influence of the changes in RH on bubble size and a better experimental control of RH are required to get a more accurate measure of the increase in emulsion flow. In all, the results of the bubble hold-up analysis show that the height to which the EF or FI internals extend may be optimised for the desired decrease in hold-up.

At first thought, one may expect the mean residence time of gas in the FI column to be shorter than the baseline case because a portion of the gas is injected higher in the column. However, this is not necessarily the case. In fact, it is expected that the mean residence time will either remain unchanged or only decrease slightly [12,15]. Even if there is a slight decrease in residence time, it is mitigated by the improved gas–solid contact resulting from the injection of gas directly into the emulsion phase, the increased driving force for mass transfer between the bubble and emulsion phases, and the increased fraction of gas in the emulsion phase. In the EF system, the reduction of bubble size, and increased flow in the emulsion phase are expected to result in an increased residence time. Detailed residence time distribution measurements will be measured in future work. In both systems, the amount of backmixing is expected to decrease, leading to more plug flow-like behaviour. Since the mass transfer from the bubble to the emulsion phase is typically the rate-limiting step in chemical conversions, it will depend on the rate of mass transfer and the rate of reaction how the combination of changes in residence times and bubble sizes will affect the conversion and selectivity of the system using the electric field enhanced fluidised bed or the distributed secondary gas injection system.

5. Conclusions

Both the electric field enhanced fluidised bed and the column with distributed secondary injection by using a fractal injector have been demonstrated to redistribute gas to smaller bubbles and to the emulsion phase. Both systems lead to an increase in particle–gas contact but differ in the mechanism by which this is achieved. In the comparison between electric fields and secondary injection, we find that the reduction of bubble size by the fractal injector is larger at higher flow rates, while the electric fields can force homogeneous fluidisation at lower flow rates. Based on the smaller bubble size, the introduction of dynamic structures by both systems is expected to yield significant increases in conversion and selectivity. However, their different influences on the residence time distributions mean that the optimum choice will differ from application to application. It remains for future experimental work that includes chemical reactions to demonstrate how the changes in bubble size and residence time can be used to the greatest advantage.

Acknowledgements

F. Kleijn van Willigen and J.R. van Ommen thank C.M. van den Bleek and J. van Turnhout for their long-term support. D. Christensen and M.-O. Coppens thank the Dutch National Science Foundation, NWO, for support via a Young Chemist award (NWO/Jonge Chemici).

References

[1] C.M. van den Bleek, M.-O. Coppens, J.C. Schouten, Chem. Eng. Sci. 57 (2002) 4763–4778.
[2] D. Kunii, O. Levenspiel, Fluidization Engineering, second ed., Butterworth–Heinemann, Boston, 1991.
[3] M.P. Dudukovic, F. Larachi, P.L. Mills, Chem. Eng. Sci. 54 (1999) 1975–1999.
[4] A. Cybulski, J.A. Moulijn, Structured Catalysts and Reactors, Dekker, New York, 1998.
[5] O. Levenspiel, Powder Technol. 122 (2002) 1–9.
[6] S. Kaart, J.C. Schouten, C.M. van den Bleek, Catal. Today 48 (1999) 185–194.
[7] J.P.K. Seville, R. Clift, Powder Technol. 37 (1984) 117–129.
[8] S.C. Saxena, W.Y. Wu, Can. J. Chem. Eng. 77 (1999) 312–318.
[9] G.M. Colver, Powder Technol. 112 (2000) 126–136.
[10] F. Kleijn van Willigen, J.R. van Ommen, J. van Turnhout, C.M. van den Bleek, Int. J. Chem. Reactor Eng. 1 (2003) A21 http://www.bepress.com/ijcre/vol1/A21.
[11] M.J. Rhodes, X.S. Wang, M. Nguyen, P. Stewart, K. Liffman, Chem. Eng. Sci. 56 (2001) 4433–4438.
[12] Y. Cheng, C.M. van den Bleek, M.-O. Coppens, in: Proceedings of 10th International Conference on Fluidisation, United Engineering Foundation, NY, 2001, pp. 373–380.
[13] J. van der Schaaf, J.C. Schouten, F. Johnsson, C.M. van den Bleek, Int. J. Multiphas. Flow 29 (2002) 865–880.
[14] F. Kleijn van Willigen, J.R. van Ommen, J. van Turnhout, C.M. van den Bleek, J. Electrostat. 63 (2005) 943–948.
[15] M.-O. Coppens, J.R. van Ommen, Chem. Eng. J. 96 (2003) 117–124.